

**NORTH PARK FARM QUARRY,
BLETCHINGLEY, SURREY**
**OPTICALLY STIMULATED LUMINESCENCE
(OSL) DATING OF A MESOLITHIC
ARCHAEOLOGICAL SITE, STAGE I**
SCIENTIFIC DATING REPORT

Richard Bailey, Nick Branch and Jonathan Stallard



Research Department Report Series 98/2007

**North Park Farm Quarry, Bletchingley, Surrey
Optically Stimulated Luminescence (OSL) Dating of a
Mesolithic Archaeological Site, Stage I**

R M Bailey, N P Branch and J Stallard

© English Heritage 2007

ISSN 1749-8775

The Research Department Report Series, incorporates reports from all the specialist teams within the English Heritage Research Department: Archaeological Science; Archaeological Archives; Historic Interiors Research and Conservation; Archaeological Projects; Aerial Survey and Investigation; Archaeological Survey and Investigation; Architectural Investigation; Imaging, Graphics and Survey, and the Survey of London. It replaces the former Centre for Archaeology Reports Series, the Archaeological Investigation Report Series, and the Architectural Investigation Report Series.

Many of these are interim reports which make available the results of specialist investigations in advance of full publication. They are not usually subject to external refereeing, and their conclusions may sometimes have to be modified in the light of information not available at the time of the investigation. Where no final project report is available, readers are advised to consult the author before citing these reports in any publication. Opinions expressed in Research Department reports are those of the author(s) and are not necessarily those of English Heritage.

**North Park Farm Quarry, Bletchingley, Surrey
Optically Stimulated Luminescence (OSL) Dating of a
Mesolithic Archaeological Site, Stage I**

R M Bailey¹, N P Branch² and J Stallard²

Summary

Eight Optically Stimulated Luminescence (OSL) dates were obtained from the Mesolithic site at North Park Farm Quarry, Surrey, to provide a chronological framework for natural and cultural events. The OSL measurements indicate that redeposited Lower Greensand material accumulated prior to Mesolithic activity between c 764–500,000 years ago and around 24,000 years ago. This process continued during the period of human activity as shown by the results from below and above an in-situ Mesolithic hearth.

Keywords

Optically Stimulated Luminescence
Mesolithic

Author's Address

¹ School of Geography, Oxford University Centre for the Environment, University of Oxford, South Parks Road, Oxford OX1 3QY.

² ArchaeoScape, Royal Holloway University of London, Department of Geography, Egham Hill, Egham TW20 0EX.

Introduction

Excavations in 2005 and 2006 at North Park Farm Quarry Mesolithic archaeological site, Bletchingley, Surrey (Site Code: NPF05; centred on National Grid Reference: TQ 331 523) by the Surrey County Archaeological Unit (SCAU) have provided a detailed record of the Mesolithic remains, which significantly enhance earlier findings (Hayman 2003). An important component of the excavation strategy was to recover samples suitable for providing an accurate and precise chronological framework for the events recorded, both natural and cultural, using optically stimulated luminescence (OSL), thermoluminescence (TL), and radiocarbon (^{14}C) dating.

The objectives of the dating programme were to:

1. Confirm the presence of *in situ* Lower Greensand at the base of the archaeological excavation areas
2. Establish the timing and duration for the accumulation of *redeposited* Lower Greensand beneath the archaeological remains
3. Provide an independent chrono-stratigraphic record for the timing and duration of Mesolithic activities
4. Establish the timing and duration for the accumulation of *redeposited* Lower Greensand above the main archaeological features (ie hearths), and beneath a well-developed soil horizon containing a mixture of Mesolithic and post-Mesolithic cultural remains.

This report summarises the findings of the first stage of the dating programme (*stage 1*), and is based upon eight OSL dates obtained from two locations at the site; hereafter known as the 'geological section' and 'hearth section (15, Area 9)'. These data have permitted an evaluation of the suitability of the technique, building upon previous work (Toms 2005), and in conjunction with the archaeological and archaeobotanical studies, will be used to make detailed recommendations for the full dating programme (*stage 2*), involving OSL, TL, and ^{14}C dating.

The Site

The site is located between the Chalk escarpment of the North Downs (*c* 230m OD), less than a kilometre to the north, and the Lower Greensand escarpment (*c* 165m OD), about two kilometres to the south (Fig 1). The intervening lower ground is underlain by the dip slope of the Lower Greensand and, to the north of that, successively by the outcrops of the Gault and the Upper Greensand. The lower ground forms a vale (loosely, the Gault vale) that extends east to west at the foot of the North Downs. The site is at a level of *c* 115m OD, on the Lower Greensand but very close to the featheredge of the overlying Gault. Although the site is within the Gault vale, it lies at a point where the ground, sloping gently away from the foot of the Chalk escarpment, forms a broad, slightly elevated watershed within the vale, with streams draining away from it to the east and west. The site is therefore on a low spur occupied by these stream heads. In detail, the site occupies a wide, shallow depression with a broadly east-west axis.

The excavation area is underlain by Lower Greensand bedrock, with the superficial geology and soils of the site exposed in the archaeological excavation and in the active quarry immediately adjacent to the site. Broadly, in the axial part of the valley-head depression noted above, the following features are generally present. At the surface a compacted, dark greyish brown, plough layer (*c* 0.3m) is present and overlies *c* 0.5m of reddish brown, compacted gritty fine sand with scattered pieces of chalk and flint, and a variety of post-Mesolithic archaeological material. In most places, this horizon is underlain by a similar but slightly darker and greyer horizon, up to 0.2m in thickness. Flint clasts, including burnt flint and Mesolithic artefacts, are present in this horizon. Below this level, the sand is much less compacted and often free-running, and predominantly light grey or white with very variable and localised patterns of dark greyish or reddish brown staining. The thickness of this

horizon is variable, and it passes down into unweathered Lower Greensand. Flint clasts, including burnt flint and Mesolithic artefacts, are present in the upper part of this horizon.

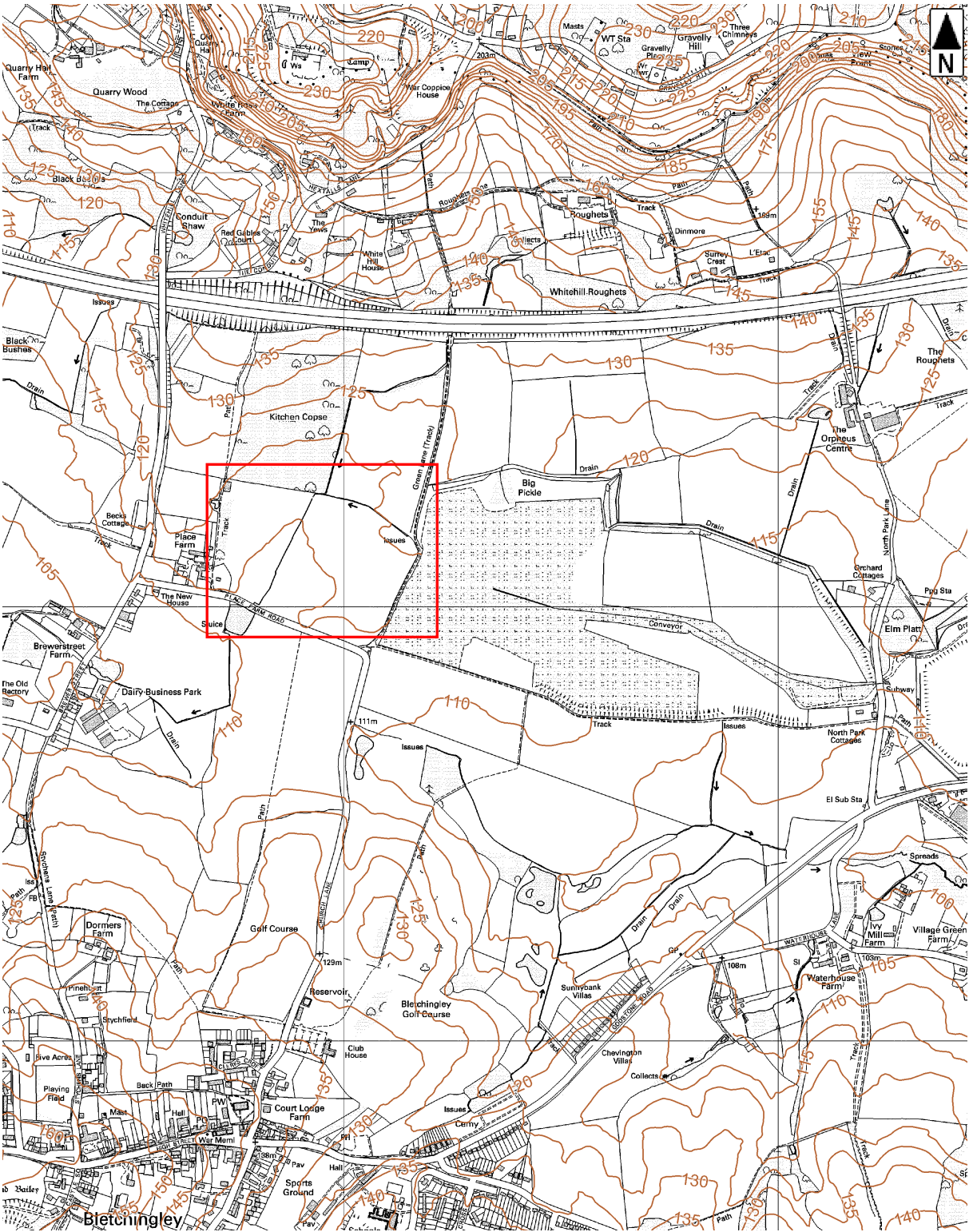


Figure 1: Location of North Park Farm, Bletchingley, Surrey.

Methods

Theoretical framework

Luminescence ages are premised upon: (1) the reduction of the datable signal – optically stimulated luminescence – within naturally occurring minerals to zero, through exposure to sunlight, and once buried, (2) the re-accumulation of this signal on exposure to natural environmental radiation from surrounding sediments, plus a small contribution from cosmic radiation. If the radiation dose rate during burial is constant in time, then the depositional age of the sediment is estimated by the expression:

$$Age = \frac{D_e}{D'}$$

Where D_e is the laboratory estimate of the total absorbed radiation dose (units Gy) and D' is the total environmental dose rate (units Gy/ka).

Field investigations

Eight samples were collected from the 'geological section' (Fig 2) and 'hearth section (15, Area 9)' (Fig 3) in daylight using opaque plastic tubing (200mm in length and 50mm in diameter). Each sample was wrapped in aluminium foil and cling film, to prevent moisture loss, and labelled. The ends of each tube were sealed with parcel tape and wrapped once more in cling film. Additional moisture content samples were collected from the rear of the cavity created by sampling. These sampling locations were selected for dating during *stage 1* because they provided an opportunity to:

1. Test the suitability of the dating method for obtaining an accurate and precise chronological framework for the events recorded, both natural and cultural
2. Test the hypothesis that *in situ* Lower Greensand is present at the base of the archaeological excavation areas
3. Establish the timing for the accumulation of *redeposited* Lower Greensand beneath the archaeological remains
4. Provide an independent chrono-stratigraphic record for the timing of Mesolithic activities
5. Establish the timing for the accumulation of *redeposited* Lower Greensand above the main archaeological features (ie hearths), and beneath a well-developed soil horizon containing a mixture of Mesolithic and post-Mesolithic cultural remains.

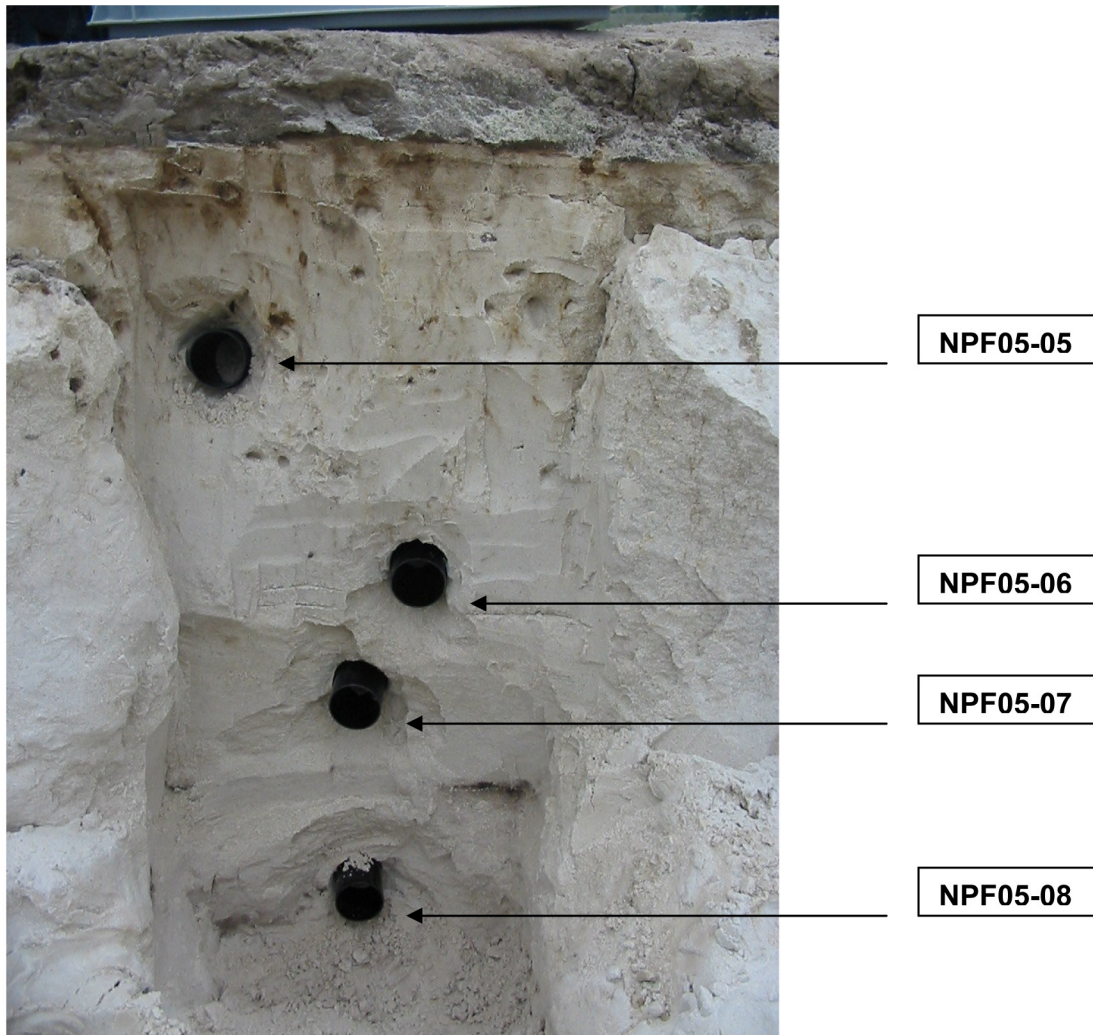


Figure 2: OSL samples NPF05-05 to NPF05-08 collected from the 'geological section' (east-facing section). Sample NPF05-08 was believed to be situated within *in situ* Lower Greensand, based on the compact nature of the sediment. Samples NPF05-07 and NPF05-06 were situated in redeposited, free-running Lower Greensand. Sample NPF05-05 was situated within a horizon of redeposited, free-running Lower Greensand thought to be broadly contemporaneous with the Mesolithic period

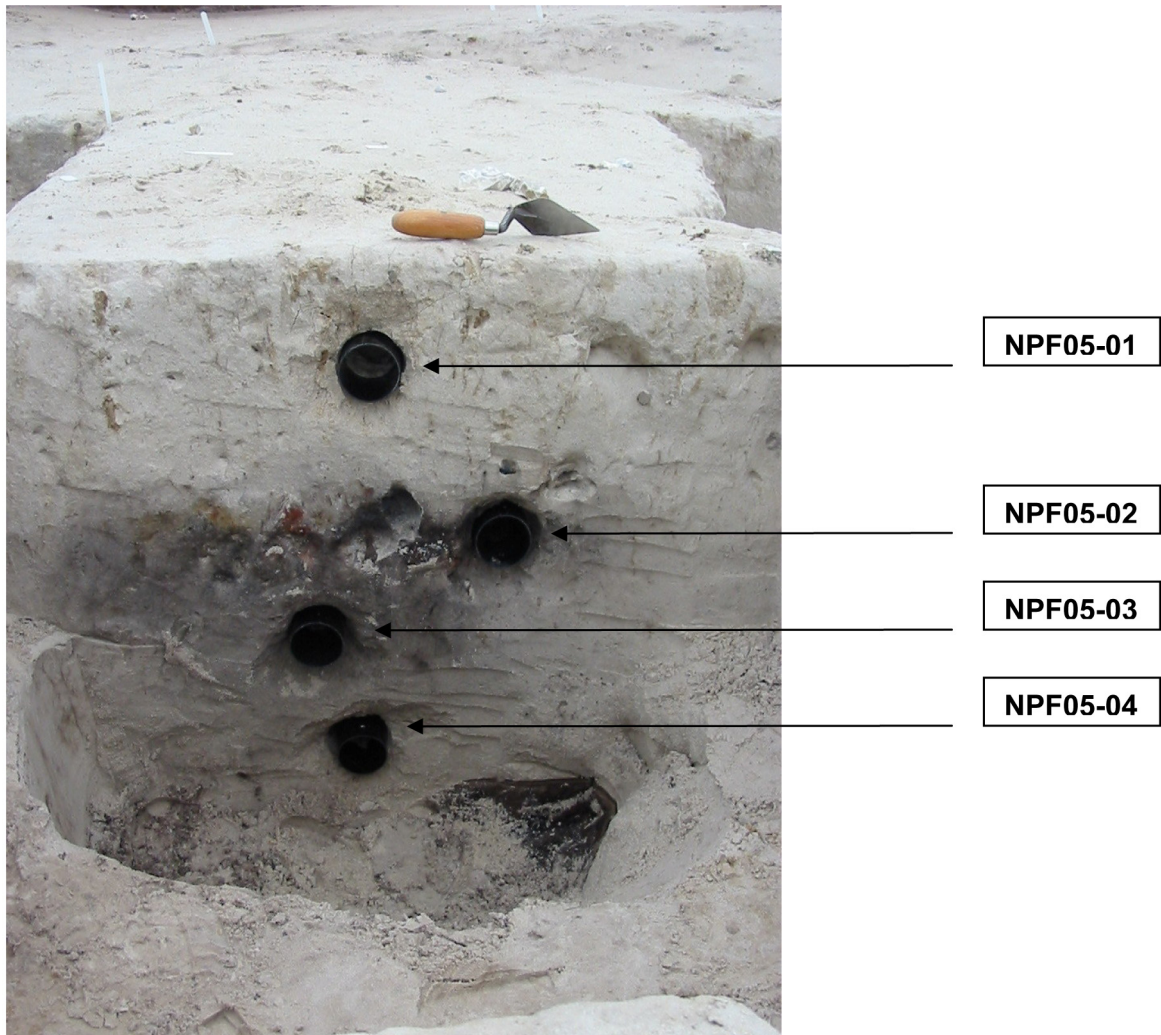


Figure 3: OSL samples NPF05-01 to NPF05-04 collected from the ‘hearth section (I5, Area 9)’ (south-facing section). Sample NPF05-04 was believed to be situated within *in situ* Lower Greensand based on the compact nature of the sediment. Samples NPF05-03 and NPF05-02 were situated in the Mesolithic hearth, which was identified by the presence of worked flint, burnt flint, and charcoal. Sample NPF05-01 was situated within a horizon of redeposited, free-running Lower Greensand, contemporaneous with the Mesolithic period, and identified by the presence of Mesolithic artefacts

Laboratory methods

D_e measurement

The ‘core’ content of each sample was dried at 40°C for 48 hours and then dry-sieved. Quartz within the fine sand (125–180µm) fraction was then isolated. This fraction was treated with 10% hydrochloric acid (HCl) and 10% hydrogen peroxide (H₂O₂) to remove the carbonate and organic components. These samples were then etched for 60 minutes in 40% hydrofluoric acid (HF), in order to remove the outer 10–15µm layer of quartz grains containing luminescence signals due to (the weakly penetrating) alpha radiation, and to remove feldspar grains. Whilst in HF, each sand sample was continuously stirred using an automated sample shaker in order to achieve isotropic etching of grains. 10% hydrochloric acid was then added to remove acid soluble fluorides. Each sample was dried, re-sieved, and quartz isolated from the remaining heavy mineral fraction using a sodium polytungstate density separation at 2.68g/cm⁻³.

Quartz was used as the dosimeter primarily because of the stability of its datable signal over the mid to late Quaternary period, predicted through isothermal decay studies (eg Smith *et al* 1990;

retention lifetime 630 Ma at 20°C) and evidenced by optical age estimates concordant with independent chronological controls (Wallinga *et al*/2001; Murray *et al*/2002; Murray and Olley 2002; Stokes *et al*/2003). This stability is in contrast to the anomalous fading of comparable signals commonly observed for other ubiquitous sedimentary minerals such as feldspar and zircon (Wintle 1973; Templer 1985; Spooner 1993).

Twenty-four multi-grain aliquots of quartz from each sample were then mounted on aluminium discs for the determination of equivalent dose values using an automated Risø reader (TL-DA-15 Reader). This large sample number was deemed necessary to provide sufficient data to assess patterns of scatter during the calculation of D_e .

Optical stimulation of luminescence was provided by filtered blue ($\lambda=470\text{nm}$) diodes mounted within the Risø reader, delivering a power at the sample of $\sim 35\text{mW/cm}^2$. Infrared stimulation, ($\lambda=885\text{nm}$, 1W/cm^2), was used to screen each sample aliquot for feldspar contamination (Hütt *et al*/1988). This diagnostic, applied to both the natural and laboratory signals (to accommodate potential fading of IRSL signals), identified no such contamination in any of the aliquots measured. Stimulated photon emissions from the quartz aliquots were measured using a high sensitivity bi-alkali photo-multiplier tube filtered by 5mm of HOYA U-340 glass filters (passing a peak centred on $\sim 360\text{nm}$).

Regenerated OSL signals were obtained by irradiation using a 40mCi $^{90}\text{Sr}/^{90}\text{Y}$ beta source incorporated within the Risø set and calibrated for 125–180 μm multi-grain aliquots of quartz against the 'Hotspot 800' ^{60}Co gamma source located at the National Physical Laboratory, UK.

D_e values were obtained through calibrating the 'natural' OSL signal, acquired during burial, against 'regenerated' optical signals obtained by administering known amounts of laboratory dose. Specifically, D_e estimates were obtained using the Single-Aliquot Regenerative-dose (SAR) protocol, as described in Wintle and Murray (2006).

Prior to measurement of the natural (L_n) or regenerated (L_x) signals, the aliquot was preheated at 260°C for 10s; a preheat of 220°C (10s) was administered prior to measurement of the corresponding test-dose signals (T_n , T_x ; test dose of 5Gy was used). During optical stimulation, aliquot temperature was maintained at 130°C.

A ratio of L_x/T_x ratios for repeated regenerative-doses was obtained for each aliquot in order to quantify the success of sensitivity correction (ideally the ratio should be unity). Zero-dose signals (expressed as the ratio $[L_x/T_x]/[L_n/T_n]$, where x denotes the zero-dose cycle in this case) were also measured, in order to assess the contribution to the measured D_e of thermal transfer. Mean D_e values are the weighted (geometric) mean D_e calculated using the central age model outlined by Galbraith *et al* (1999) and are quoted at 1σ confidence (standard error).

Environmental dose rate (D') and age calculation

The mean dose rate to each sediment sample was derived from measurements of U, Th, and K concentrations made using Inductively Coupled Plasma Mass Spectrometry (ICP-MS), with conversions to dose rate made using dose rate conversion factors given in Adamiec and Aitken (1998), β -attenuation factors of Mejdahl (1979), and the relevant absorption coefficients to correct for the presence of water in the sediment given by Zimmerman (1971). Estimates of cosmic dose followed the calculations of Prescott and Hutton (1994).

Errors on all values used in the expanded age equation (both random and systematic) were combined to give the overall uncertainty in each age estimate (errors were combined using standard methods in which the partial derivative of each relevant term is multiplied by its error and added in quadrature to accumulate the total error). The quoted error on the resultant luminescence age estimates is a 1σ standard error.

The measured concentrations of Thorium, Potassium, and Uranium were found to be relatively low at North Park Farm, yielding an overall dose rate of approximately 30% of that typical found in such locations. A full record of the ICP-MS data and subsequent dosimetric calculations can be found in Tables 1 and 2.

Results

Equivalent dose results

The equivalent dose (D_e) results for each sample are given in the dating summary table (Table 2). Six out of the eight samples showed the expected level of inter-aliquot scatter (overdispersion values of ~10%) and no significant skew, indicating that incomplete bleaching is unlikely to have influenced the results. Two of the samples (NPF05-02 and NPF05-03) showed more considerable levels of scatter, however, and significant positive skew of the D_e values. In these two cases the (three-parameter) Minimum-age model of Galbraith *et al* (1999) was used to estimate the most likely value of D_e . Example data sets are shown in Figure 4. The D_e value of sample NPF05-04 (169Gy), and hence its age, is substantially higher than that of the other three samples within this context. The reason for this is not clear, but probably reflects the sampling of 'geological age' *in situ* or moderately reworked Lower Greensand. Samples NPF05-06, NPF05-07, and NPF05-08 also yielded relatively high D_e values, which again most probably reflects the location of the boundary between the *in situ* Lower Greensand and the redeposited Lower Greensand.

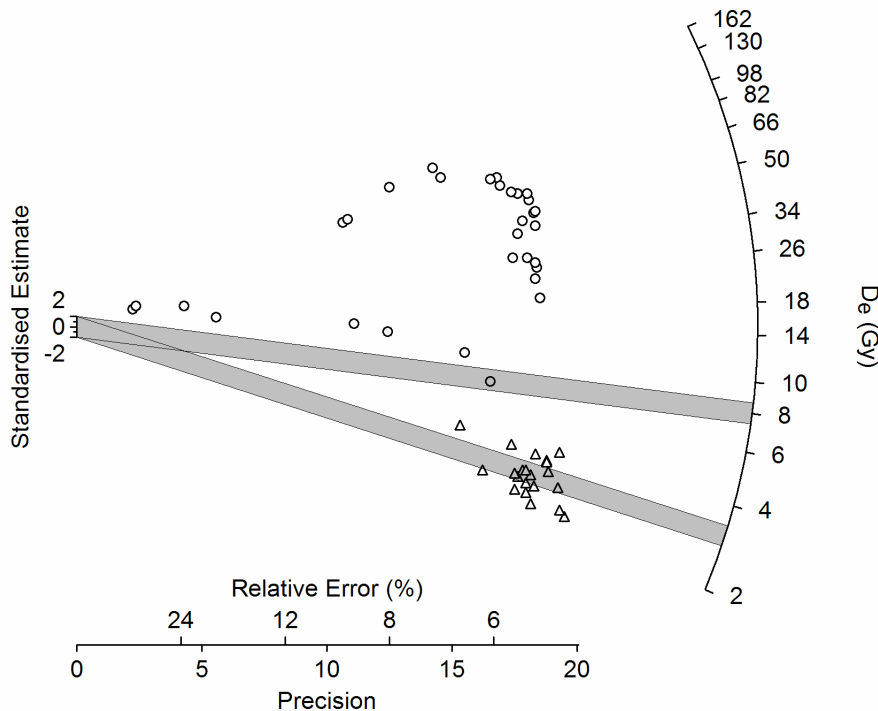


Figure 4: Radial plot showing equivalent dose (D_e) estimates for sample NPF05-01 (triangles) and NPF05-03. The grey bars indicate the sample D_e values in each case (see Table 2)

Inductively Coupled Plasma Mass Spectrometry (ICP-MS) Results

Table 1a: ICP-MS data for samples NPF05-01 to NPF05-08 (% and ppm)

| Sample | SiO ₂ | Al ₂ O ₃ | Fe ₂ O ₃ | MgO | CaO | Na ₂ O | K ₂ O | TiO ₂ | P ₂ O ₅ | MnO | Ba | Co | Cr | Cu | Li |
|----------|------------------|--------------------------------|--------------------------------|------|------|-------------------|------------------|------------------|-------------------------------|-------|----|----|----|----|----|
| NPF05-01 | 99.15 | 0.31 | 0.34 | 0.01 | 0.03 | 0.01 | 0.02 | 0.08 | 0.01 | 0.002 | 23 | 0 | 11 | 3 | 1 |
| NPF05-02 | 99.47 | 0.21 | 0.34 | 0.01 | 0.00 | 0.01 | 0.01 | 0.10 | 0.00 | 0.002 | 22 | 0 | 10 | 3 | 1 |
| NPF05-03 | 99.94 | 0.22 | 0.31 | 0.01 | 0.00 | 0.01 | 0.01 | 0.07 | 0.00 | 0.001 | 20 | 1 | 8 | 3 | 1 |
| NPF05-04 | 99.58 | 0.18 | 0.33 | 0.01 | 0.00 | 0.01 | 0.01 | 0.08 | 0.01 | 0.002 | 23 | 0 | 8 | 5 | 1 |
| NPF05-05 | 99.29 | 0.18 | 0.50 | 0.01 | 0.03 | 0.01 | 0.01 | 0.08 | 0.00 | 0.003 | 22 | 1 | 8 | 3 | 1 |
| NPF05-06 | 99.73 | 0.18 | 0.35 | 0.09 | 0.02 | 0.01 | 0.01 | 0.09 | 0.00 | 0.002 | 23 | 0 | 10 | 3 | 1 |
| NPF05-07 | 99.64 | 0.18 | 0.30 | 0.01 | 0.00 | 0.00 | 0.01 | 0.05 | 0.00 | 0.001 | 19 | 1 | 7 | 3 | 1 |
| NPF05-08 | 99.64 | 0.24 | 0.37 | 0.01 | 0.00 | 0.00 | 0.01 | 0.08 | 0.00 | 0.002 | 22 | 1 | 9 | 5 | 1 |

(continued)

| Sample | Ni | Sc | Sr | V | Zn | Zr | Pb | U | Th | Rb | Nb | Cs | Hf | Ta | Tl |
|----------|----|----|----|---|----|-----|----|------|------|----|-----|------|------|------|------|
| NPF05-01 | 4 | 1 | 7 | 0 | 3 | 158 | 3 | 0.31 | 0.64 | 1 | 3.5 | 0.13 | 3.74 | 0.29 | 0.09 |
| NPF05-02 | 3 | 0 | 5 | 0 | 4 | 272 | 4 | 0.46 | 0.76 | 1 | 3.8 | 0.12 | 6.48 | 0.31 | 0.08 |
| NPF05-03 | 3 | 0 | 5 | 0 | 3 | 100 | 6 | 0.25 | 0.53 | 2 | 2.2 | 0.30 | 2.54 | 0.16 | 0.08 |
| NPF05-04 | 3 | 0 | 5 | 1 | 4 | 146 | 4 | 0.28 | 0.64 | 1 | 2.8 | 0.13 | 3.60 | 0.16 | 0.09 |
| NPF05-05 | 3 | 0 | 5 | 1 | 4 | 138 | 5 | 0.34 | 0.45 | 1 | 2.6 | 0.12 | 3.32 | 0.18 | 0.08 |
| NPF05-06 | 8 | 0 | 6 | 0 | 4 | 155 | 5 | 0.30 | 0.56 | 2 | 3.1 | 0.14 | 3.92 | 0.23 | 0.07 |
| NPF05-07 | 3 | 0 | 5 | 1 | 3 | 89 | 3 | 0.24 | 0.37 | 1 | 1.8 | 0.12 | 2.30 | 0.13 | 0.08 |
| NPF05-08 | 3 | 0 | 5 | 0 | 4 | 177 | 5 | 0.33 | 0.58 | 1 | 2.8 | 0.15 | 4.29 | 0.20 | 0.11 |

(continued)

| Sample | Y | La | Ce | Pr | Nd | Sm | Eu | Gd | Dy | Ho | Er | Yb | Lu | Mo |
|----------|---|-----|-----|-----|-----|------|------|------|------|------|------|------|------|-----|
| NPF05-01 | 3 | 6.9 | 5.7 | 0.5 | 2.1 | 0.42 | 0.10 | 0.44 | 0.37 | 0.10 | 0.25 | 0.50 | 0.07 | 0.8 |
| NPF05-02 | 3 | 2.9 | 4.7 | 0.4 | 1.7 | 0.43 | 0.10 | 0.41 | 0.45 | 0.11 | 0.31 | 0.61 | 0.09 | 0.5 |
| NPF05-03 | 2 | 2.3 | 3.5 | 0.4 | 1.4 | 0.36 | 0.08 | 0.27 | 0.28 | 0.07 | 0.21 | 0.40 | 0.04 | 0.6 |
| NPF05-04 | 3 | 2.5 | 4.2 | 0.4 | 1.5 | 0.40 | 0.08 | 0.32 | 0.40 | 0.09 | 0.28 | 0.52 | 0.07 | 0.5 |
| NPF05-05 | 2 | 2.7 | 4.2 | 0.4 | 1.6 | 0.41 | 0.07 | 0.34 | 0.35 | 0.09 | 0.23 | 0.41 | 0.08 | 0.5 |
| NPF05-06 | 3 | 3.1 | 4.9 | 0.5 | 1.9 | 0.46 | 0.08 | 0.36 | 0.38 | 0.08 | 0.23 | 0.47 | 0.07 | 0.5 |
| NPF05-07 | 2 | 3.1 | 4.7 | 0.4 | 1.7 | 0.40 | 0.08 | 0.32 | 0.27 | 0.06 | 0.20 | 0.36 | 0.06 | 0.4 |
| NPF05-08 | 3 | 3.1 | 4.8 | 0.5 | 1.7 | 0.49 | 0.10 | 0.30 | 0.31 | 0.08 | 0.27 | 0.46 | 0.07 | 0.5 |

Dating Results

Table 2: Summary data used for age calculation

| Sample number | NPF05-01 | NPF05-02 | NPF05-03 | NPF05-04 | NPF05-05 | NPF05-06 | NPF05-07 | NPF05-08 |
|---|--------------|--------------|--------------|---------------|-------------|---------------|---------------|---------------|
| Age (ka) | 10.58 | 23.75 | 24.09 | 630.54 | 9.65 | 505.15 | 764.2 | 568.38 |
| error (ka) | 0.93 | 1.75 | 1.98 | 50.07 | 0.81 | 41.49 | 194.61 | 48.25 |
| De (Gy) | 3.15 | 7.97 | 7.32 | 168.66 | 2.83 | 129.14 | 215 | 161.56 |
| uncertainty | 0.14 | 0.35 | 0.35 | 7.7 | 0.13 | 6.36 | 53 | 10.12 |
| Grain size | | | | | | | | |
| Min grain size (µm) | 180 | 180 | 180 | 180 | 180 | 180 | 180 | 180 |
| Max grain size (µm) | 250 | 250 | 250 | 250 | 250 | 250 | 250 | 250 |
| Measured concentrations | | | | | | | | |
| standard fractional error | 0.05 | 0.05 | 0.05 | 0.05 | 0.05 | 0.05 | 0.05 | 0.05 |
| % K | 0.008 | 0.008 | 0.017 | 0.008 | 0.008 | 0.008 | 0.008 | 0.008 |
| error (%K) | 0 | 0 | 0.001 | 0 | 0 | 0 | 0 | 0 |
| Th (ppm) | 0.64 | 0.76 | 0.64 | 0.53 | 0.45 | 0.37 | 0.56 | 0.58 |
| error (ppm) | 0.032 | 0.038 | 0.032 | 0.027 | 0.023 | 0.019 | 0.028 | 0.029 |
| U (ppm) | 0.28 | 0.46 | 0.31 | 0.25 | 0.34 | 0.24 | 0.3 | 0.33 |
| error (ppm) | 0.014 | 0.023 | 0.016 | 0.013 | 0.017 | 0.012 | 0.015 | 0.017 |
| Cosmic dose calculations | | | | | | | | |
| Depth (m) | 1.11 | 1.47 | 1.325 | 1.685 | 1.3 | 1.795 | 1.61 | 2.05 |
| error (m) | 0.1 | 0.1 | 0.1 | 0.1 | 0.1 | 0.1 | 0.1 | 0.1 |
| Average overburden density (g.cm ³) | 2 | 2 | 2 | 2 | 2 | 2 | 2 | 2 |
| error (g.cm ³) | 0.1 | 0.1 | 0.1 | 0.1 | 0.1 | 0.1 | 0.1 | 0.1 |
| Latitude (deg), north positive | 51 | 51 | 51 | 51 | 51 | 51 | 51 | 51 |
| Longitude (deg), east positive | 0 | 0 | 0 | 0 | 0 | 0 | 0 | 0 |
| Altitude (m OD) | 100 | 100 | 100 | 100 | 100 | 100 | 100 | 100 |
| Geomagnetic latitude | 77.6 | 77.6 | 77.6 | 77.6 | 77.6 | 77.6 | 77.6 | 77.6 |
| Dc (µGy/ka), 55°N, 0km altitude | 0.18 | 0.171 | 0.175 | 0.166 | 0.175 | 0.164 | 0.168 | 0.158 |
| error | 0.021 | 0.017 | 0.018 | 0.015 | 0.018 | 0.015 | 0.016 | 0.014 |
| Cosmic dose rate (Gy/ka) | 0.185 | 0.176 | 0.179 | 0.171 | 0.18 | 0.168 | 0.172 | 0.162 |
| error | 0.021 | 0.017 | 0.019 | 0.016 | 0.019 | 0.015 | 0.016 | 0.014 |
| Moisture content | | | | | | | | |
| Moisture (water/ wet sediment) | 0.031 | 0.042 | 0.052 | 0.052 | 0.035 | 0.021 | 0.058 | 0.024 |
| error | 0.02 | 0.02 | 0.02 | 0.02 | 0.02 | 0.02 | 0.02 | 0.02 |
| Total dose rate (Gy/ka) | 0.3 | 0.34 | 0.3 | 0.27 | 0.29 | 0.26 | 0.28 | 0.28 |
| error | 0.02 | 0.02 | 0.02 | 0.02 | 0.02 | 0.02 | 0.02 | 0.02 |
| % error | 7.58 | 5.92 | 6.66 | 6.5 | 6.98 | 6.57 | 6.39 | 5.73 |
| Age (ka) | 10.58 | 23.75 | 24.09 | 630.54 | 9.65 | 505.15 | 764.2 | 568.38 |
| error | 0.93 | 1.75 | 1.98 | 50.07 | 0.81 | 41.49 | 194.61 | 48.25 |
| % error | 8.78 | 7.37 | 8.2 | 7.94 | 8.35 | 8.21 | 25.47 | 8.49 |

The results of the OSL dating (Figs 5, 6, and 7) indicate that:

1. The eight samples, obtained from two locations at the site, provide a stratigraphically consistent chronological framework, with an increase in age with sample depth (Figs 5, 6, and 7)
2. *In situ* Lower Greensand is not present at the base of the archaeological excavation areas examined during *stage 1* (Figs 5 and 6).
3. *Redeposited* Lower Greensand accumulated beneath the archaeological remains during possibly four depositional events, at approximately 764,000, 630,000, 568,000 and 505,000 years ago (Figs 5 and 6).
4. *Redeposited* Lower Greensand also accumulated beneath the archaeological remains during the upper Palaeolithic period, at approximately 24,000 years ago (Fig 6)
5. *Redeposited* Lower Greensand continued to accumulate during the Mesolithic period, and above the main archaeological feature in the 'hearth section (15, Area 9)' (Figs 5 and 6).

The presence of OSL dates of upper Palaeolithic age from samples NPF05-02 and NPF05-03 (Figs 6 and 7) was unexpected, given their proximity to the hearth. We suggest that these dates may be derived from sand from underneath the original hearth, which was deposited during the upper Palaeolithic, but which has become 'stained' by the downward movement of dark, fine particulate matter, mainly charcoal, from the hearth. The observed size and shape of the hearth may therefore be somewhat misleading from the photographic record (Figs 6 and 7), and possibly confined to a thinner layer above, and to the left of, samples NPF05-02 and NPF05-03.

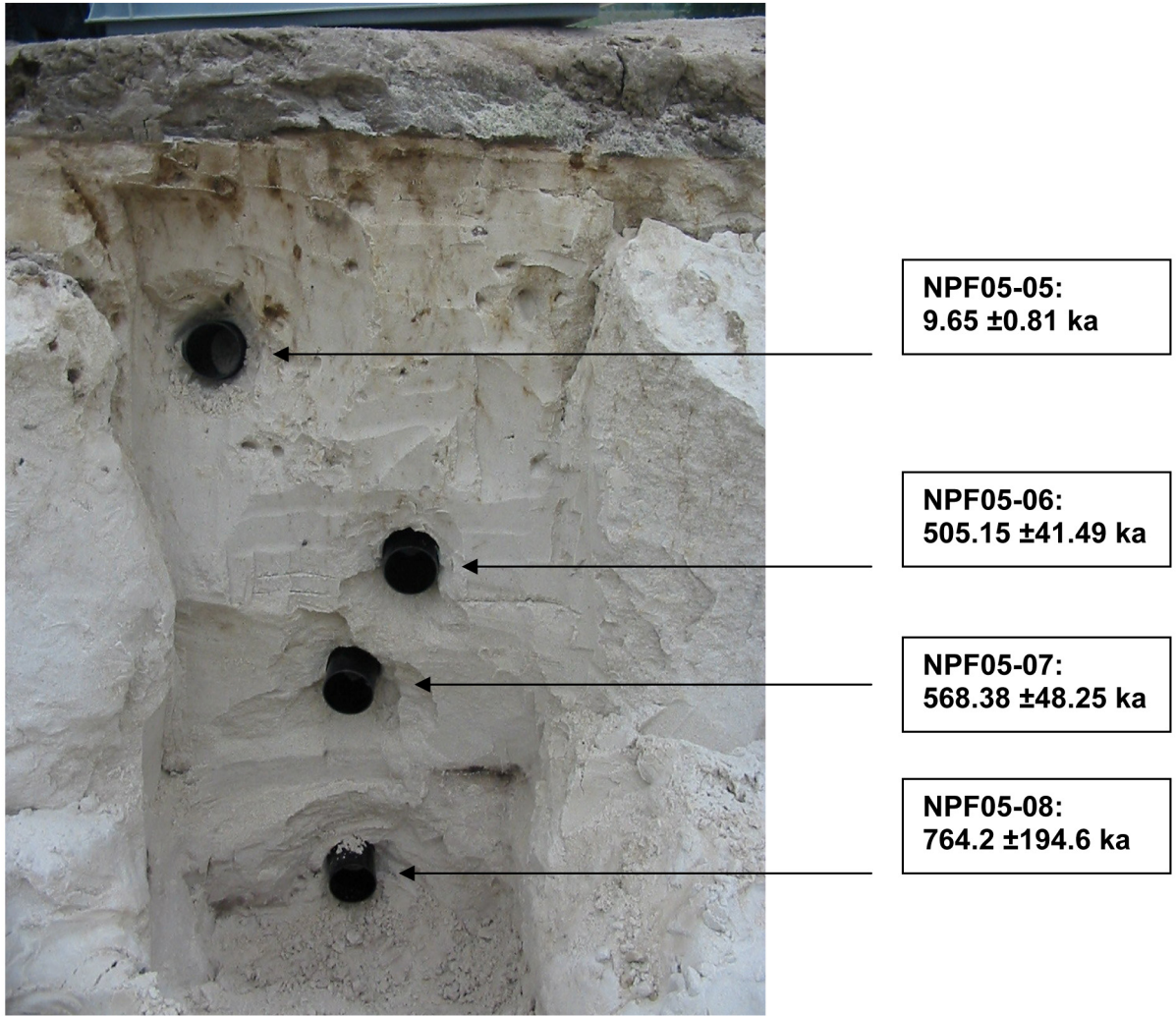


Figure 5: OSL ages for samples NPF05-05 to NPF05-08 from the 'geological section'

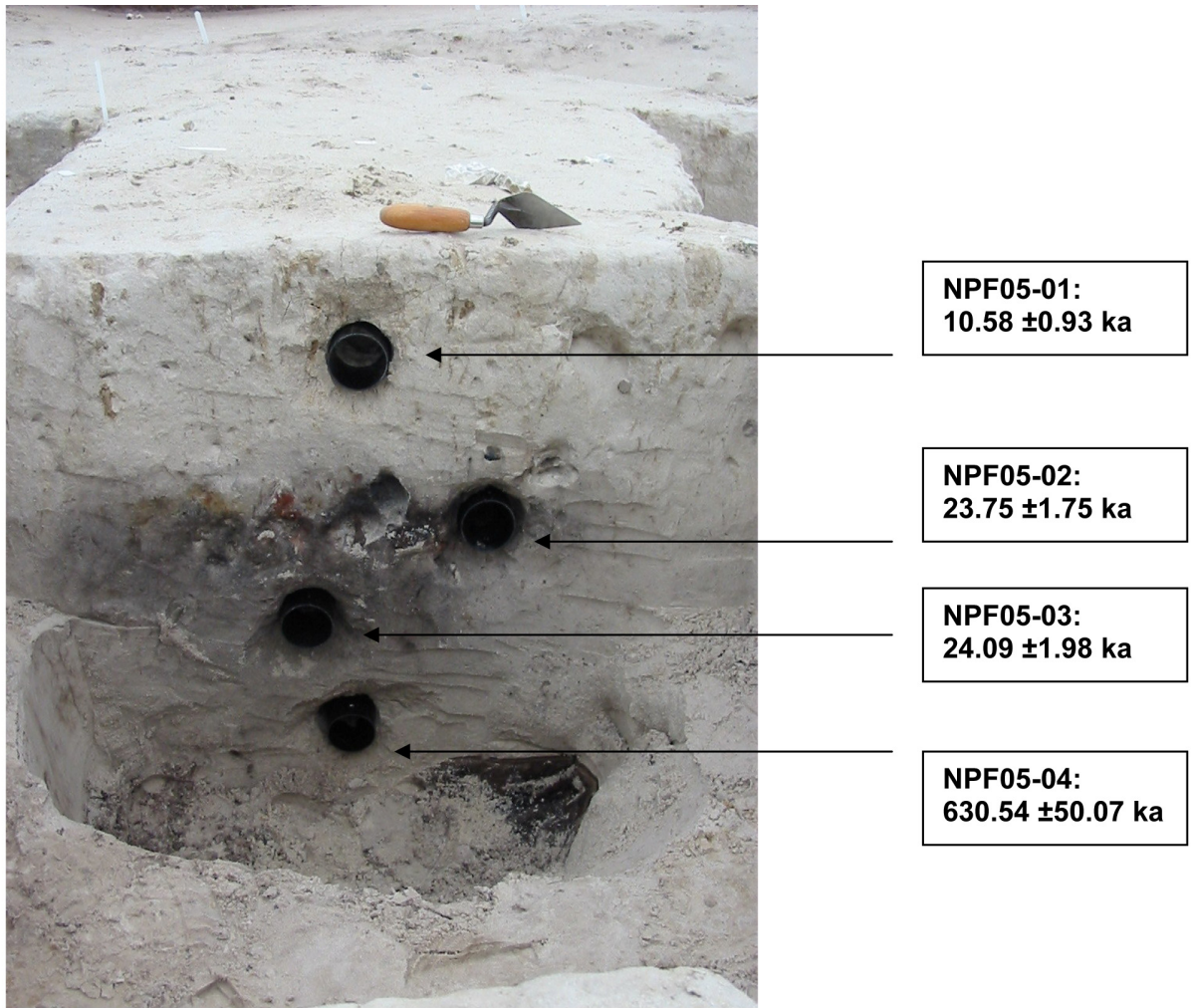


Figure 6: OSL ages for samples NPF05-01 to NPF05-04 from the 'hearth section (15, Area 9)'

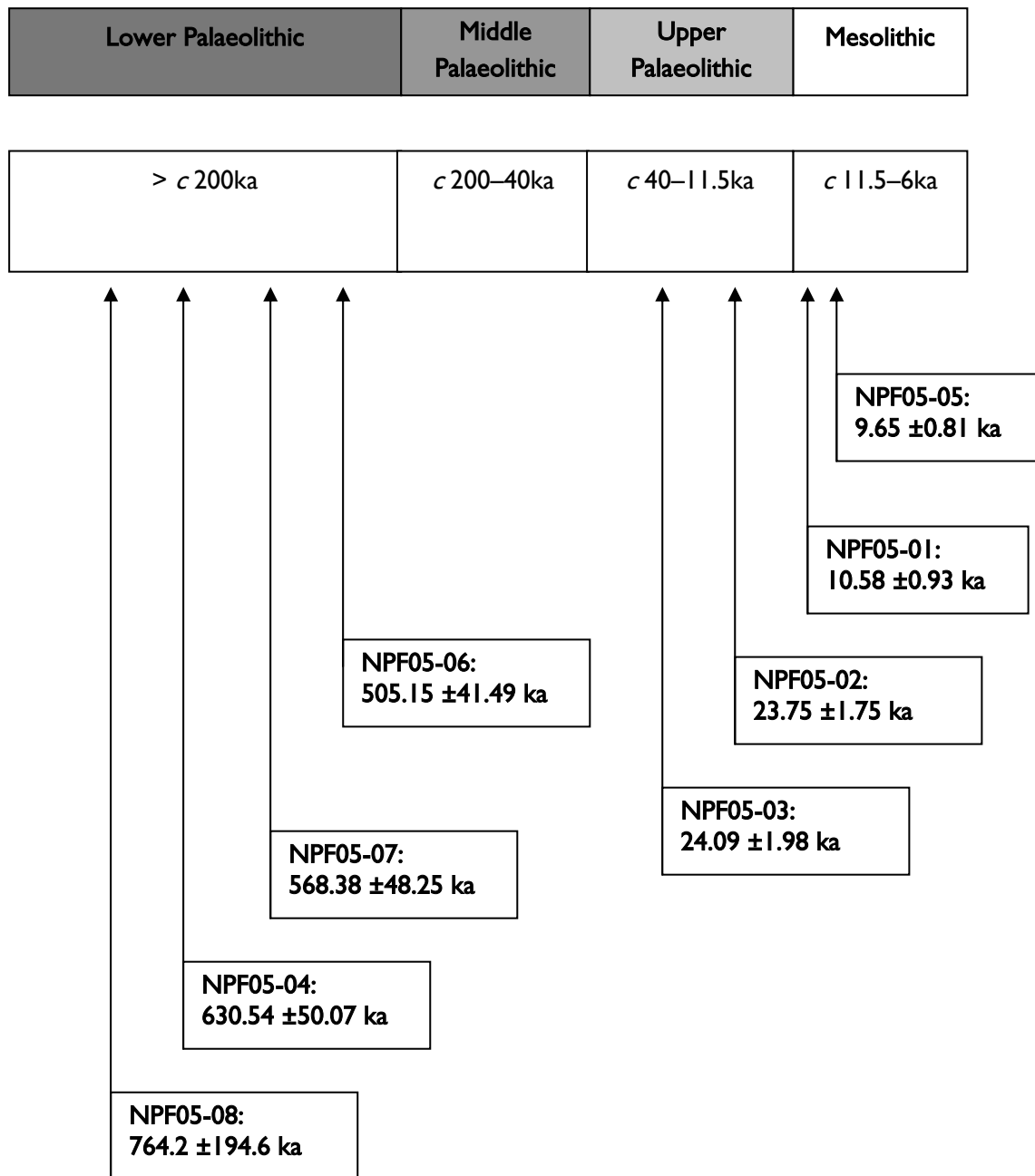


Figure 7: Results of the OSL dating at North Park Farm Quarry

References

- Adamiec, G, and Aitken, M J, 1998 Dose-rate conversion factors: new data, *Ancient TL*, **16**, 37–50
- Galbraith, R F, Roberts, R G, Laslett, G M, Yoshida, H, and Olley, J M, 1999 Optical dating of single and multiple grains of quartz from Jinmium rock shelter (northern Australia): Part I, Experimental design and statistical models, *Archaeometry*, **41**, 339–64
- Hayman, G N, 2003 *An archaeological evaluation of the Mesolithic hollow at North Park Farm, near Bletchingley, Surrey (NPF02)*, unpubl rep, Surrey County Archaeological Unit
- Hütt, G, Jaek, I, and Tchonka, J, 1988 Optical dating: K-feldspars optical response stimulation spectra, *Quat Sci Rev*, **7**, 381–6
- Mejdahl, V, 1979 Thermoluminescence dating: beta-dose attenuation in quartz grains. *Archaeometry*, **21**, 61–72
- Murray, A S, and Olley, J M, 2002 Precision and accuracy in the Optically Stimulated Luminescence dating of sedimentary quartz: a status review, *Geochronometria*, **21**, 1–16
- Murray, A S, Wintle, A G, and Wallinga, J, 2002 Dose estimation using quartz OSL in the non-linear region of the growth curve, *Radiation Protection Dosimetry*, **101**, 371–4
- Prescott, J R, and Hutton, J T, 1994 Cosmic ray contributions to dose rates for luminescence and ESR dating: large depths and long-term time variations, *Radiation Measurements*, **23**, 497–500
- Smith, B W, Rhodes, E J, Stokes, S, Spooner, N A, 1990 The optical dating of sediments using quartz, *Radiation Protection Dosimetry*, **34**, 75–8
- Spooner, N A, 1993 'The validity of optical dating based on feldspar', unpubl D Phil thesis, Oxford Univ
- Stokes, S, Ingram, S, Aitken, M J, Sirocko, F, and Anderson, R, 2003 Alternative chronologies for late Quaternary (Last Interglacial-Holocene) deep sea sediments via optical dating of silt-sized quartz, *Quat Sci Rev*, **22**, 925–41
- Templer, R H, 1985 The removal of anomalous fading in zircons, *Nuclear Tracks and Radiation Measurements*, **10**, 531–7
- Toms, P S, 2005 *Luminescence dating for the Bletchingley excavations, Surrey*, Centre for Archaeol Rep **9/2005**
- Wallinga, J, Murray, A S, Duller, G A T, and Tornqvist, T E, 2001 Testing optically stimulated luminescence dating of sand-sized quartz and feldspar from fluvial deposits, *Earth and Planetary Sci Letters*, **193**, 617–30
- Wintle, A G, 1973 Anomalous fading of thermoluminescence in mineral samples, *Nature*, **245**, 143–4
- Zimmerman, D W, 1971 Thermoluminescent dating using fine grains from pottery, *Archaeometry*, **13**, 29–52